Talanta 103 (2013) 20–27

Contents lists available at SciVerse ScienceDirect

Talanta

journal homepage: www.elsevier.com/locate/talanta

Standoff Raman spectrometry for the non-invasive detection of explosives precursors in highly fluorescing packaging

Emad L. Izake [a,*], Shankaran Sundarajoo [a], William Olds [a], Biju Cletus [a], Esa Jaatinen [b], Peter M. Fredericks [a]

[a] Chemistry Discipline, Faculty of Science and Technology, Queensland University of Technology, 2 George St., Brisbane, QLD 4001, Australia
[b] Physics Discipline, Faculty of Science and Engineering, Queensland University of Technology, 2 George St., Brisbane, QLD 4001, Australia

ARTICLE INFO

Article history:
Received 29 August 2012
Received in revised form
25 September 2012
Accepted 25 September 2012
Available online 27 October 2012

Keywords:
Deep Raman spectroscopy
Highly fluorescing packaging
Standoff detection
Explosives precursors
Homeland security

ABSTRACT

Noninvasive standoff deep Raman spectroscopy has been utilised for the detection of explosives precursors in highly fluorescing packaging from 15 m. To our knowledge this is the first time standoff deep Raman spectroscopy of concealed substances in highly fluorescing coloured packaging is demonstrated. Time-resolved Raman spectroscopy, spatially offset Raman spectroscopy and time-resolved spatially offset Raman spectroscopy have been compared to identify their selectivity towards the deep layers of a sample. The selectivity of time-resolved Raman spectroscopy towards the concealed chemical substances was found to be comparable to that of spatially offset Raman spectroscopy. However, time-resolved Raman spectroscopy did not require precise translation of the laser excitation beam onto the surface of the interrogated packaging as in the case of spatially offset Raman spectroscopy. Our results confirm that standoff time-resolved spatially offset Raman spectroscopy has significantly higher selectivity towards the deep layers of a sample when compared to the other deep Raman spectroscopy modes. The developed spectrometer was capable of detecting the concealed substances within 5 s of data acquisition. By using time-resolved spatially Raman spectroscopy, a Raman spectrum that is representative of the content alone was acquired without the use of sophisticated algorithms to eliminate the spectral contributions of the packaging material within the acquired spectrum as in the case of time-resolved Raman spectroscopy and spatially offset Raman spectroscopy.

1. Introduction

Modern forensic and national security investigations of hazardous substances such as explosive precursors, illicit substances and chemical warfare require analytical platforms that can conduct rapid analysis of solid, liquid and gaseous samples with high accuracy, sensitivity and chemical specificity. In many situations it is required to detect hazardous substances that are hidden in diffusely scattering packaging from a safe standoff distance to avoid potential risks to the investigating personnel. The analysis is required to be noninvasive while maintaining the hazardous substance undisturbed within its own packaging. Raman spectroscopy has been recently demonstrated as a noninvasive detection technique that is capable of meeting those requirements [1]. Standoff direct Raman spectroscopy has been demonstrated for the detection of surface deposits from different distances. Several literature that describe standoff direct Raman spectroscopy and its various applications have been published recently [2–18]. In this technique, a laser excitation beam is focused onto the exposed particles of the suspected substance. The collection optics are aligned to collect the backscattered photons from the excited spot. Standoff direct Raman spectroscopy was not successful in detecting chemical substances that are hidden in diffusely scattering opaque packaging. This is because of the fact that Raman spectra when detected in the backscatter geometry are always overwhelmed with fluorescence and Raman photons from the surface layer (e.g. packaging material). The significant amount Raman and fluorescence photons from the surface layer overwhelm the acquired spectrum and may mask the Raman signals from the deeper layers (e.g. chemical substance) of the sample [19]. Kim et al. applied a wide-area illumination scheme to screen pharmaceutical formulations in translucent plastic packaging by direct Raman spectroscopy [20]. The wide-area illumination scheme was used to average out the surface layer irregularities. However, the acquired spectra were still heavily dominated by Raman spectral lines from the polymer material.

When depth-resolved information is required, Raman spectroscopy is an ideal candidate since excitation photons can penetrate the sample to interact with different layers and the interactions

* Corresponding author. Tel.: +61 7 3138 2501; fax: +61 7 3138 1804.
E-mail addresses: ekiriakous@hotmail.com, e.kiriakous@qut.edu.au (E.L. Izake).

0039-9140/$ - see front matter © 2012 Elsevier B.V. All rights reserved.
http://dx.doi.org/10.1016/j.talanta.2012.09.055

can be monitored and used to collect analytical information of the different layers [21,22]. Deep Raman spectroscopy has been demonstrated recently as a viable Raman spectroscopy technique for the standoff detection of concealed substances [22–25]. In deep Raman spectroscopy, the Raman spectra from the deep layers are recorded while the Raman and fluorescence radiation from the surface layer are suppressed [22–25]. The suppression of the surface layer Raman and fluorescence radiation can be achieved by space resolve as in spatially offset Raman spectroscopy (SORS) [26]. In SORS, a spot on the surface of the sample is excited with a laser beam and the generated Raman photons are collected from another spot that offset by a distance (ΔS) from a laser-excited spot. When a laser beam interacts with a sample that consists of a diffusely-scattering surface layer and a deep layer (e.g. a chemical substance), the excitation photons propagate into the deeper layer in a random walk-like fashion. Due to the random scattering of the photons within the deep layers of the sample, the excited area within the sample bulk increases with the increase in the sample depth [24,26,28]. When the collection of the return light is carried out at an offset point from the excitation spot, the return radiation will be relatively rich with Raman photons from the deep layer [26]. Therefore the acquired spectrum becomes indirectly enriched with Raman photons from the deeper layers of the sample and the Raman spectrum of the surface layer is suppressed [26,28]. On the other hand, the radiation collected at zero offset from the excitation spot will be rich with Raman and fluorescence photons from the surface layer. To reveal the true spectrum of the deep layer by SORS, at least 2 Raman spectra must be detected at zero and ΔS offsets. Scaled subtraction of the acquired signals is then carried out using sophisticated algorithms to eliminate the residual spectral contributions of the surface layer [24,26,28]. The need to apply sophisticated multivariate statistical treatments to the SORS Raman spectra constitute a disadvantage to the technique when used in forensic and national security investigations where maintaining the integrity of the original measurements is a key requirement by the legal system. SORS has been demonstrated for biomedical applications [29,30], pharmaceutical analysis [31,32], forensic and national security investigations [33,34]. In these applications SORS was used to screen samples from a short distance of 6 cm. Zachhuber et al. recently extended SORS to standoff measurements of concealed chemical substances from distances up to 12 m [24]. Standoff pulsed SORS required precise translation of the excitation beam onto the sample surface to different offset points from the collection system [24,25]. The demonstrated pulsed standoff SORS utilised gated detection instead of non-gated detection as in conventional continuous wave SORS. Since gated CCD's are noisier than conventional non-gated CCD counterparts, conventional continuous wave SORS have inherently better signal to noise characteristics than pulsed standoff SORS.

An alternative technique to selectively detect spectra from the deep layers of a sample is time-resolved Raman spectroscopy (TRRS) [35–38]. TRRS can be used to acquire selective chemical information from the deep layers of a system that has a diffusely scattering surface layer [36,37]. When the excitation beam interacts with a sample, the Raman and fluorescence photons from the surface layer are generated almost spontaneously. These photons spend minimum travel time to arrive at the detector when compared to the time required by the emitted photons from deeper layers. This is because the Raman photons from the deeper layers experience multiple scattering events while travelling from the bulk of the sample to its surface and consequently arrive at the detector after a time delay. By using gated detection the time delay experienced by the deep layers photons while travailing towards the detector can be utilised to exclude the detection of the majority of Raman and fluorescence photons that are emitted from the surface layer especially when the fluorescence is shorter than the migration time of photons within the deep layer. This can be achieved by carefully synchronizing the detector gate to become active after the majority of the photons emitted from the surface layer have passed the detector [35–37]. Therefore the acquired TRRS spectrum becomes enriched with photons from the deeper layers relative to those from the surface layer. TRRS involves the use of pulsed laser excitation and gated detection (ICCD) where the voltage driving the detector gate is triggered by the laser pulse through a delay generator and every point in time, before, during and after the pulse, can be measured. Therefore, the time-resolved Raman spectrum of different phases within a sample can be studied by shifting the detector gate delay in time [39]. Matousek et al. demonstrated time-resolved Raman spectroscopy for profiling deep layers using picosecond Kerr gating [40]. However their technique was instrumentally complex and only suited laboratory applications [24]. Petterson et al. recently demonstrated the application of time-resolved Raman spectroscopy for the noninvasive screening of chemical substances behind polymer material from a non-contact working range [41]. They used picosecond laser excitation and narrow detector gate of 250 ps, that was delayed several hundred picoseconds after the laser pulse, to allow for efficient temporal discrimination between photons from the surface of the sample and those from the deeper layers. Using a very narrow gate width caused the signal intensity to be significantly reduced and, therefore, resulted in a low signal to noise ratio (SNR). The low SNR may preclude the detection of chemical substances of weak Raman activity. Zachhuber et al. recently demonstrated a TRRS spectrometer that uses long laser pulses for the sample excitation [42]. They used the developed spectrometer for the standoff of substances that were concealed in a white polymer container where they applied detector gate delays up to 330 ns.

Time-resolved spatially offset Raman spectroscopy (TR-SORS) has been demonstrated recently as a combined space and time-resolved Raman spectroscopy technique that has high selectivity towards the deep layers [37]. In time-resolved SORS the excitation is carried out by a short laser pulse (picoseconds laser). For the purpose of suppressing the Raman and fluorescence photons from the surface layer, a very narrow detector gate width is used [37]. The return light is detected from an offset position from the excitation spot by a gated detector. The detector gate is delayed in time to avoid the detection of the majority of the Raman and fluorescence photons from the surface layer and, at the same time, detect the Raman photons from the deeper layers of the sample [25,37,43]. Therefore, by using a proper gate delay, it is possible to discriminate against the return photons from the surface layer and selectively detect the Raman signal from the deeper layers. We recently demonstrated TR-SORS for the non-invasive detection of concealed chemical substances that are concealed opaque packaging [25,43,44].

The aim of this new study is to extend the application of deep Raman spectroscopy to the standoff detection of energetic substances in highly fluorescing opaque packaging (coloured packaging). To our knowledge, this is the first time standoff deep Raman spectroscopy is demonstrated for the detection of hidden explosives precursors in coloured packaging. We also study the selectivity of the deep Raman spectroscopy techniques (SORS, TRRS and TR-SORS) standoff TRRS towards the deep layers of a sample. Our results confirm that, TRRS and SORS have comparable selectivity towards the deep layers of a sample while TR-SORS have significantly higher selectivity when compared to the other two techniques. Contrary to TRRS and SORS, multivariate statistical treatments were not required to develop a TR-SORS spectrum that represents the deep layer alone. This significant

advantage of TR-SORS make the technique of value to forensic and homeland security applications where unambiguous identification of the concealed hazardous substance is a critical requirement of the law enforcement and legal systems. To our knowledge, this is the first detailed study that investigates and compares the selectivity of the various standoff deep Raman spectroscopy techniques towards the deep layers of a sample. The developed spectrometer was capable of detecting the concealed hazardous substances within 5 s of data acquisition.

2. Experimental

2.1. Chemicals

Ammonium nitrate (NH_4NO_3 $\geq$98%), nitromethane (CH_3NO_2 $\geq$98%), 2,4-dinitrotoluene ($CH_3C_6H_3(NO_2)_2$ $\geq$97%) and hydrogen peroxide (H_2O_2 30% w/v) from Sigma were screened by the unit. For sample measurements, Hydrogen peroxide and DNT were concealed within a white opaque container made of high-density polyethylene (HDPE) (with a wall thickness of 1.5 mm). Ammonium nitrate was concealed within a canary yellow HDPE container (with a wall thickness of 1.5 mm).

2.2. Instrumentation and measurements

A schematic diagram of the developed spectrometer is shown in Fig. 1. The spectrometer consisted of a 532 nm Q-switched Nd:YAG laser excitation source (Brilliant EaZy, Quantel, USA). The second harmonic laser source has a pulse length of 4 ns and a repetition rate of 10 Hz. The Raman collection system consisted of an eight inch Schmidt-Cassegrain telescope (Celestron, USA) and a long pass filter (Semrock, USA) to block the back scattered excitation laser at 532 nm. The filtered return light was collected via a fibre-optical bundle cable consisting of nineteen 200 μm diameter optical fibres (Princeton Instruments, USA) into an Acton standard series SP-2300 imaging spectrograph. The bundle was directly coupled to the slit of the spectrograph. The Raman light was detected by a PIMAX 1024RB ICCD camera (Princeton Instruments, USA). For sample measurements, 50 laser pulses of 35 mJ laser energy were focused on an area of 20 mm^2 on the sample surface. The sample measurement time was 5 s and 20 accumulations per measurement were recorded. Nitromethane was concealed in a white opaque HPDE container and screened using standoff SORS where the excitation beam was translated onto the container wall surface to different offset distances of 0, 6, 11 and 15 mm from the telescope field of view. The offset was adjusted by using a rotating mirror (mirror B in Fig. 1). For the SORS measurements, the ICCD gate was not shifted in time. This is to say that the detector was operated in the gated mode but the initial gate at which a Raman spectrum is detected was not further shifted in time (no gate delay). This experimental setting was adopted to replicate the standoff pulsed SORS detection that was demonstrated by Zachhuber et al. [23]. For the TRRS measurements, the triggering of the excitation laser pulse was first set to overlap with the opening of the detector gate then the 4 ns detector gate was progressively shifted in time using steps of 50 ps to increment the delay.

In order to test the spectrometer for the detection of explosive precursors in highly fluorescing packaging, ammonium nitrate was concealed in a yellow HDPE container and screened from an 8 m standoff distance using TRRS, SORS and TR-SORS modes. The TRRS were carried out at various detector gate delays while aligning the collection system to a zero offset from the excited spot. The SORS measurements were carried out at 0, 10, 20, 30, 40 and 50 mm spatial offsets. For the TR-SORS measurements at each spatial offset, the detector gate was progressively shifted in time using increments of 50 ps. Prior to each Raman measurement, the used HDPE container was thoroughly rinsed with ethanol, acetone and distilled water to maintain the outer surface of the used packaging free of any contamination. Each of the Raman measurements reported in this study was repeated 6 times (n=6).

3. Results and discussions

3.1. Change in the Raman spectral profile of the sample with the spatial offset and the detector gate delay

In order to study the change in the Raman spectrum of the sample with the change in the spatial offset and the change in the gated delay, nitromethane was concealed in a white opaque HDPE plastic container and used as a model for screening by both techniques. The measurements were carried out at 15 m standoff distance. The results are shown in Fig. 2a,b. The top sub-plots of Fig. 2a,b represents the Raman spectra that were collected by SORS and TRRS at zero spatial offset and zero detector gate delay respectively. The spectra showed distinctive Raman signals at 1036, 1138, 1306 and 1450 cm^{-1} from the HDPE polymer and Raman signals at 653 and 920 cm^{-1} from the nitromethane content. As indicated by the figure, it was impossible to discriminate between the surface layer and the content of the sample without prior knowledge of the Raman spectral signatures of the HDPE polymer and the nitromethane content. However, by increasing the spatial offset (in SORS measurements) or shifting the detector gate in time (in TRRS measurements) noticeable changes in the spectral profile of the sample occur where the band intensities at 1036, 1138, 1306 cm^{-1} and 1450 cm^{-1} decrease sharply and experience significant suppression. To the contrary, the band intensities at 653, 920 cm^{-1} increase till they become the prominent spectral lines within the acquired SORS or TRRS spectrum (bottom sub plots in Fig. 2a,b). By monitoring the change in the relative intensities of the Raman bands with the increase in the spatial offset or detector gate delay, it became possible to discriminate the Raman spectrum of the nitromethane content from that of the HDPE polymer without prior knowledge of the HDPE polymer Raman fingerprint. This is significant for forensic and homeland investigations of explosives substances

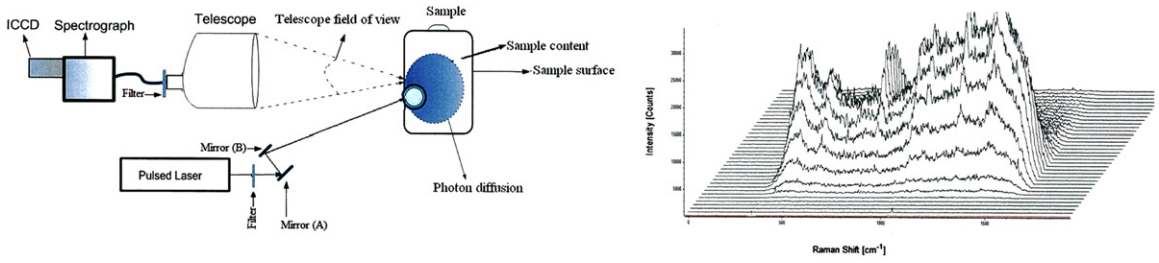

Fig. 1. Schematic diagram of the developed deep Raman spectrometer for the standoff detection of concealed substances.

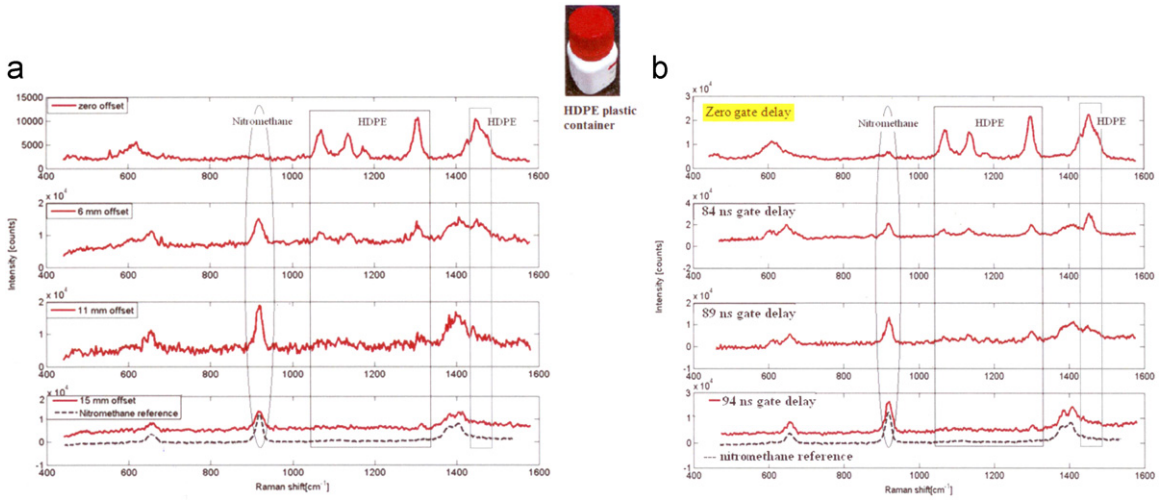

Fig. 2. Standoff Raman spectra of nitromethane concealed in an opaque HDPE plastic container (a) standoff SORS measurements at 15 m (*SNR*=9.20) and (b) standoff TRRS measurements at 15 m (*SNR*=8.70).

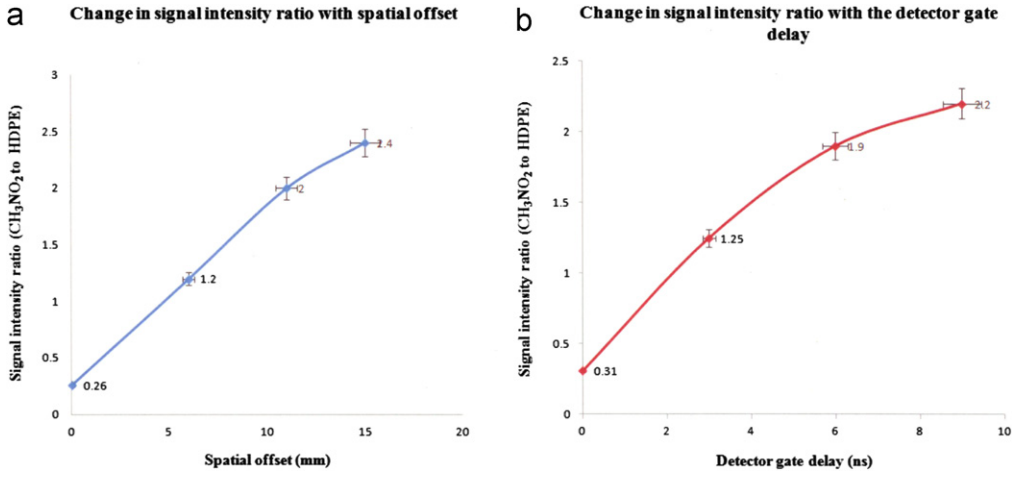

Fig. 3. Change in the signal intensities ratio of nitromethane (at 920 cm^{-1}) to HDPE plastic material (at 1303 cm^{-1}) with (a) the change in the spatial offset (standoff SORS detection mode) and (b) the change in detector gate delay (standoff TRRS).

hidden in suspicious packaging where the chemical composition of the packaging material is usually unknown.

3.2. Selectivity of time-resolved Raman spectroscopy towards deep layers

We recently reported the selectivity of the TR-SORS towards the deep layers of a sample in comparison to that of SORS [25]. In this new study, we extended our investigation to determine the selectivity of TRRS towards the deep layers within a sample. We compared the selectivity of TRRS towards the deep layers of a sample to that of SORS. We calculated the signal intensity ratio of nitromethane (at 920 cm^{-1}) to the HDPE polymer (at 1303 cm^{-1}) in the TRRS and SORS spectra that were detected from a standoff distance of 15 m. The change in the signal intensity ratio with the spatial offset (SORS mode) and the detector gate delay (TRRS mode) is shown in Fig. 3a,b. As indicated by the figure, the change in the intensity ratio (CH_3NO_2 to HDPE) was comparable in both SORS and TRRS spectra. Both techniques were capable of detecting the Raman spectrum nitromethane. However the TRRS, SORS spectra still showed a Raman signal from the HDPE polymer at 1303 cm^{-1} (bottom sub plots in Fig. 2a,b). For the TRRS spectrum of nitromethane at 94 ns detector gate delay, the signal to noise ratio (S/N) was 9.20. For the SORS spectrum of nitromenane at 15 mm spatial offset, the S/N was 8.70. The low signal to noise ratio observed in the SORS spectrum can be attributed in part to the fact that the Raman signal was collected from an offset point to the laser-excited spot. This leads to a relative reduction of the acquired Raman signal intensity due to the relatively low population of Raman photons arriving at the detector [26,27].

3.3. Standoff time-resolved Raman spectroscopy (TRRS) measurements

When the excitation laser beam interacts with the surface of a sample, Raman and fluorescence photons are generated. Since fluorescence occurs with a time constant on the order of 10^{-9} s from excitation, whereas Raman is almost spontaneous, therefore Raman scattering and fluorescence emissions occur in distinctly separate time frames when the laser pulse duration is shorter than the fluorescence lifetime [45–47]. For a diffusely-scattering two-layer sample, the Raman photons from the surface layer have relatively narrow distribution, whereas the Raman signal emerging from deeper within the sample has broader distribution in time, and is less intense than that developed from the surface [35–37]. Due to the multiple scattering events that the deep layer

Raman photons experience within the bulk of the sample, they photons emerge at the surface of the sample and arrive at the detector after a time delay when compared to the Raman and fluorescence photons from the surface layer. The natural delay of the deep layer photons can be used to resolve the deep layer Raman photons from the surface photons. By shifting the ICCD detector gate in time, the detection of the majority of the Raman and fluorescence photons from the surface layer can be suppressed (not detected). In addition, when a proper gate delay is used, the detection can be synchronized with the arrival of the delayed Raman photons of the deep layer [35–42]. We used the developed spectrometer for the detection of 30% H_2O_2 and 2,4-DNT in white opaque HDPE plastic container by TRRS from a standoff distance of 15 m (Fig. 4a,b). The SNR in the TRRS spectra of 2,4-DNT and H_2O_2 were 21.30 and 8.70 respectively. The success of using TRRS in detecting H_2O_2 indicated the potential of the technique for detecting peroxide-based explosives from a safe standoff distance.

3.4. Standoff SORS vs TRRS vs TR-SORS

We used the developed spectrometer for the standoff detection ammonium nitrate in a canary yellow HDPE container from an 8 m standoff distance by TRRS, SORS and TR-SORS modes. The SORS spectra at various offsets are shown in Fig. 5a. The signal intensity ratio of ammonium nitrate (at 1011 cm^{-1}) to HDPE (at 1568 cm^{-1}) in the SORS measurements changed from 0.70 at zero offset to 1.10 at 10 mm offset to 2.20 at 20 mm offset. The TRRS spectra of ammonium nitrate in the yellow container at various detector gate delays are shown in Fig. 5b. The signal intensity ratio (ammonium nitrate to HDPE) changed from 0.44 at 35 ns gate delay to 0.90 at 44 ns gate delay to 1.90 at 50 ns gate delay respectively. These results confirmed that both TRRS and SORS have comparable selectivity towards the deep layer of the sample. The acquired TRRS spectrum at 50 ns detector gate delay and the SORS spectrum at 20 mm spatial offset were still showing a Raman signal of the HDPE polymer at 1568 cm^{-1}. To eliminate the interference from the HDPE material into the TRRS and the SORS spectra, multivariate statistical treatment of the spectra must be applied. For example, to obtain a TRRS spectrum that is a representative of the ammonium nitrate content alone, it was necessary to carry out a scaled subtraction between the TRRS spectra that were collected at 35 ns and 50 ns detectors gate delay (Fig. 6).

For the standoff detection of the concealed ammonium nitrate using TR-SORS, the Raman collection system was offset by 20 mm from the laser-excited spot onto the surface of the container. The TR-

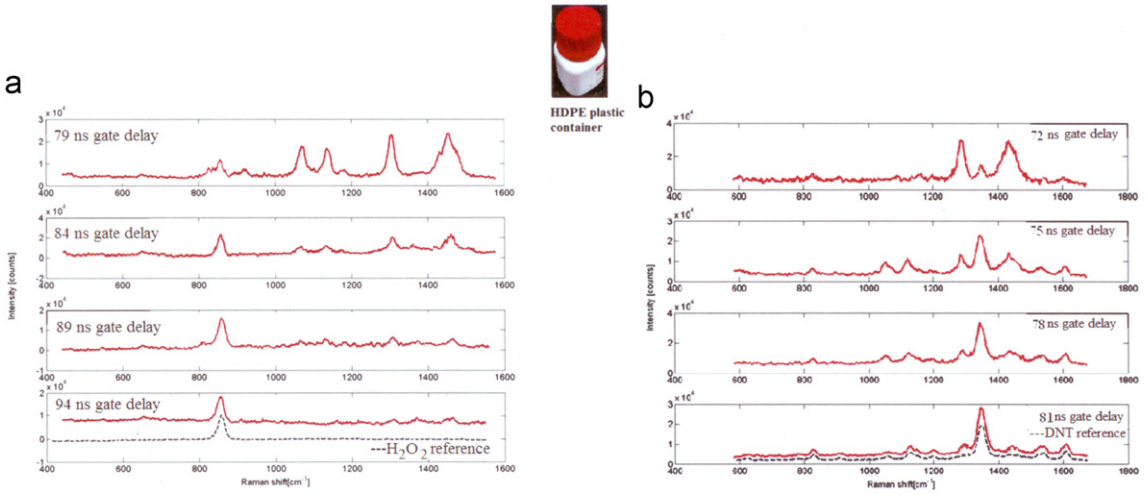

Fig. 4. Standoff TRRS measurements of (a) 30% v/v hydrogen peroxide solution (*SNR*=8.70), (b) 2,4-DNT (*SNR*=21.30). The chemical substances were concealed in a white opaque HDPE plastic container and measurements carried out from standoff distance of 15 m.

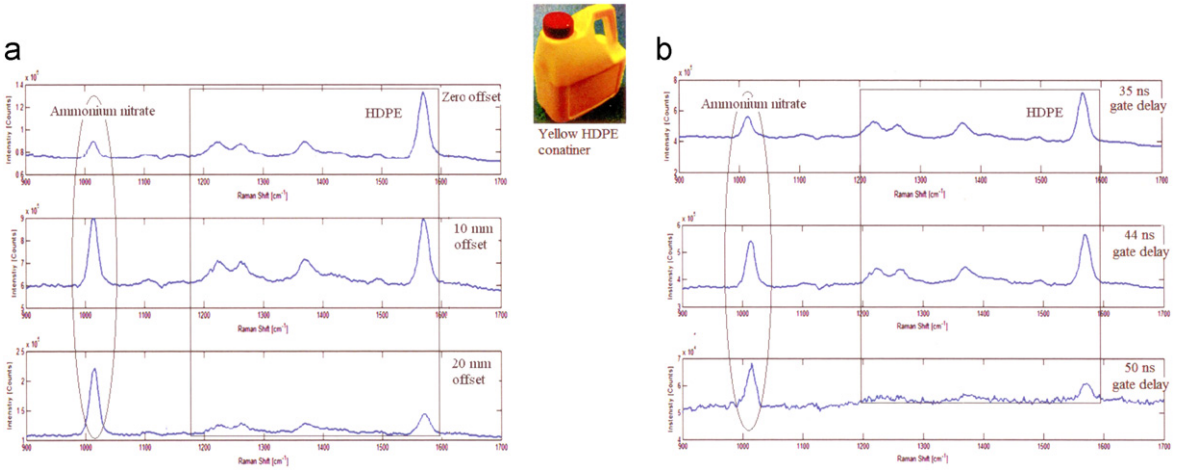

Fig. 5. Standoff detection of ammonium nitrate by (a) SORS at different spatial offsets (b) TRRS at different detectors gate delay. The chemical substance was concealed in an opaque yellow HDPE plastic container and measurements carried out from standoff distance of 8 m.

SORS spectra at various detector gate delays are shown in Fig. 7. The signal intensity ratio (ammonium nitrate to HDPE) in the TR-SORS spectra changed from 2.10 at 41 ns gate delay to 3.20 at 44 ns gate delay to 4.50 at 50 ns detector gate delay. The TR-SORS spectrum of ammonium nitrate at 50 ns gate delay and 20 mm spatial offset (bottom subplot in Fig. 7) did not show any residual Raman signal from the HDPE polymer when compared to that obtained by SORS and TRRS. Therefore there was no need to use any sophisticated algorithms to obtain a TR-SORS spectrum that represents the ammonium nitrate content alone. This is a significant advantage of TR-SORS when compared to both TRRS and SORS techniques. To further confirm the selectivity of TR-SORS towards the deep layers of a sample, we carried out standoff TR-SORS screening of ammonium nitrate in the yellow container at 10, 20, 30, 40, 50 mm offsets. In these tests the detector gate delay was changed progressively from zero ns gate delay to 50 ns gate delay. The signal intensity ratio (ammonium nitrate to HDPE) was found to change significantly with the change in the detector gate delay and the spatial offset to reach a maximum of 65 at 50 ns gate delay and 50 mm spatial offset (Fig. 8). The results in Fig. 8 suggested that the spatial offset contributed significantly to the selectivity of the TR-SORS technique towards the deep layers of the sample. To test this outcome, we re-screened ammonium nitrate in the yellow HDPE container by spatially offset Raman spectroscopy at 50 mm offset without introducing a time delay to the detector gate. The detector was operated in the gated mode and its gate was not shifted in time from the initial value at

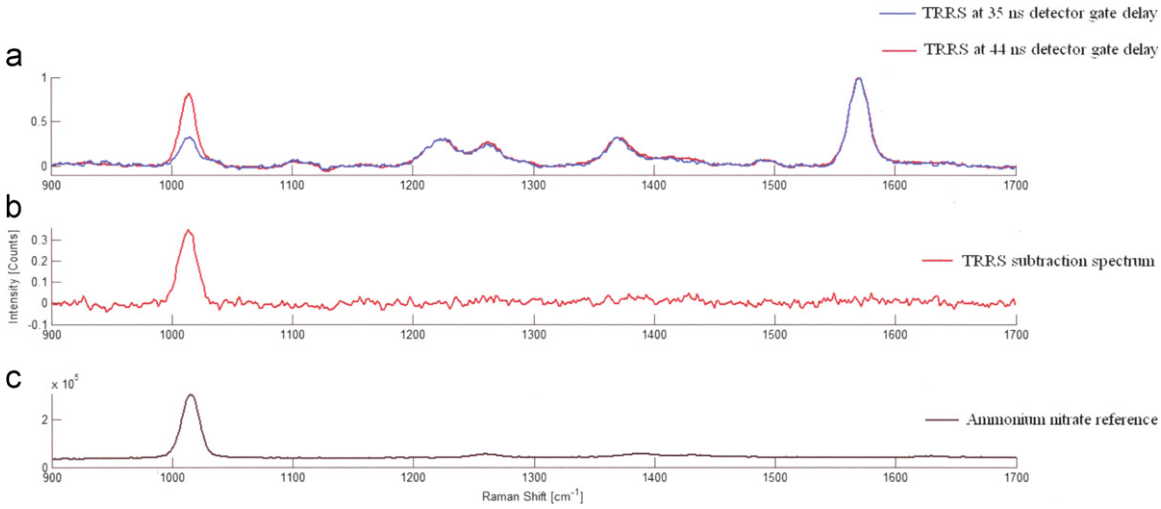

Fig. 6. Standoff detection of ammonium nitrate by (a) TRRS at 35 ns and 44 ns detector gate delays, (b) scale-subtracted TRRS spectrum of ammonium nitrate, (c) ammonium nitrate Raman reference spectrum. The chemical substance was concealed in an opaque yellow HDPE plastic container and measurements carried out from standoff distance of 8 m.

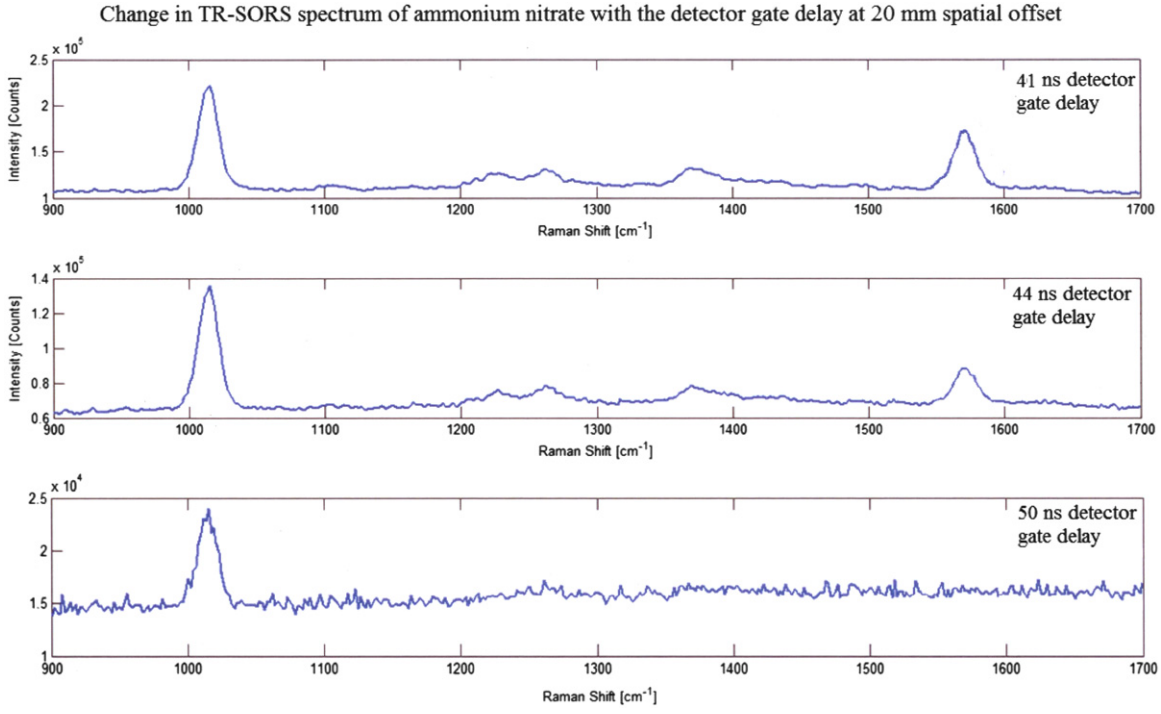

Fig. 7. Change in the TR-SORS spectrum of ammonium nitrate with the change in the detector gate delay. The chemical substance was concealed in an opaque yellow HDPE plastic container and measurements carried out from standoff distance of 8 m. The spatial offset between the laser-excited spot and the collection zone was kept constant at 20 mm while shifting the detector gate delay in time from 41 ns to 50 ns.

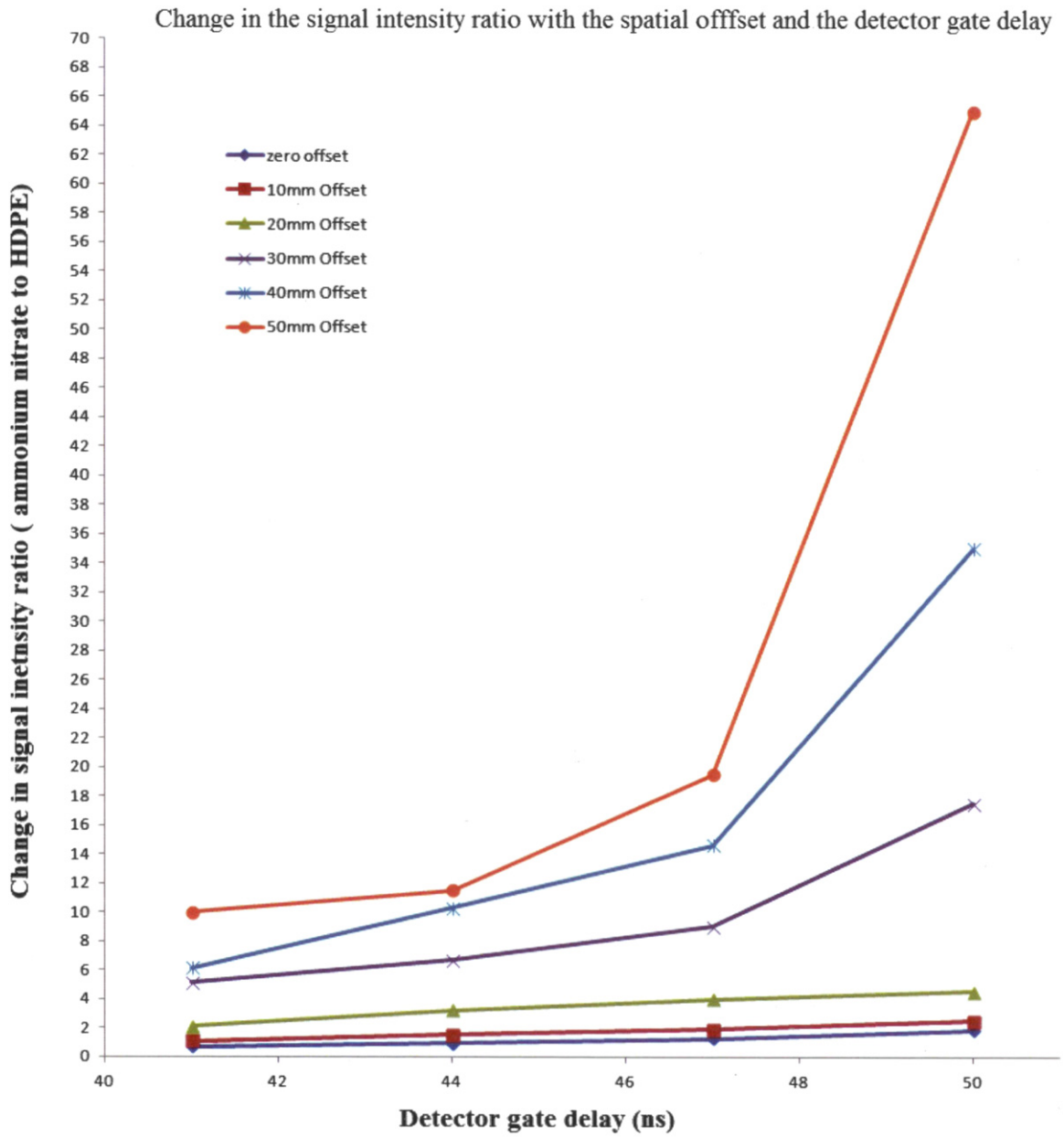

Fig. 8. Change in the TR-SORS signal intensity ratio with the change in the spatial offset and the detector gate delay. The TR-SORS measurements were carried out on ammonium nitrate in a yellow HDPE container from a standoff distance of 8 m. The signal intensity ratio of NH_4NO_3 (at 1011 cm^{-1}) to HDPE polymer at (1568 cm^{-1}) is plotted against the detector gate delay at various spatial offsets.

which the first sample Raman spectrum was detected (i.e. no gate delay was introduced). The signal intensity ratio (ammonium nitrate to HDPE) in this measurement was found to reach 7.90 only. The above results confirmed that TR-SORS has a high selectivity towards deep layer of a sample. The selectivity of TR-SORS towards the deep layers of a sample is achieved by combining both time and space resolve and is superior to that achieved by using time (TRRS) or space (SORS) resolve alone [25,43,44].

4. Conclusions

Deep Raman spectroscopy has been utilised to the standoff detection of concealed substances in highly fluorescing coloured packaging. The Raman signature of the concealed content can be identified within the acquired deep Raman spectrum (SORS, TRRS or TR-SORS) without prior knowledge of the packaging material. This can be achieved by monitoring the change in the Raman spectrum profile of the sample with the shift of the detector gate in time or the change in the spatial offset between the excitation laser beam and the Raman collection system. The selectivity of time-resolved Raman spectroscopy towards the deep layer of a sample is comparable to that of spatially offset Raman spectroscopy. However the signal to noise ratio in the TRRS spectra is higher than that in the SORS spectra. The selectivity of TR-SORS towards the deep layer of a sample is higher by orders of magnitude than that of TRRS or SORS alone. Therefore superior selectivity towards the deep layers of a sample is achieved by combining time and space resolve. By using TR-SORS, a Raman spectrum that is a representative of the sample content alone can be acquired without any multivariate treatment of the collected spectra as in the cases of TRRS and SORS. The developed spectrometer has powerful applications in national security and forensic investigations.

Acknowledgements

This work is supported by the National Security Science and Technology scheme (Department of the Prime Minister and Cabinet, Australian Government), the Queensland Government (National and International Research Alliance Partnerships scheme), the Australian Future Forensics Innovation Network (AFFIN), the Queensland Health Forensic Scientific Services and the Australian Federal Police and Health Sciences Authority Singapore.

References

[1] E.L. Izake, Forensic Sci. Int. 202 (2010) 1–8.
[2] M. Wu, M. Ray, K.H. Fung, M.W. Ruckman, D. Harder, A.J. Sedlacek, Appl. Spectrosc. 54 (2000) 800–806.
[3] M.D. Ray, A.J. Sedlacek, M. Wu, Rev. Sci. Instrum. 71 (2000) 3485–3489.
[4] S.K. Sharma, S.M. Angel, M. Ghosh, H.W. Hubble, P.G. Lucey, Appl. Spectrosc. 56 (2002) 699–705.
[5] J.C. Carter, S.M. Angel, M. Lawrence-Snyder, J. Scaffidi, R.E. Whipple, J.G. Reynolds, Appl. Spectrosc. 59 (2005) 769–775.
[6] S.K. Sharma, A.K. Misra, B. Sharma, Spectrochim. Acta 61 (2005) 2404–2412, Part A..
[7] S.K. Sharma, A.K. Misra, P.G. Lucey, S.M. Angel, C.P. McKay, Appl. Spectrosc. 60 (2006) 871–876.
[8] A. Pettersson, I. Johansson, S. Wallin, M. Nordberg, H. Östmark, Propellants Explos. Pyrotech. 34 (2009) 297–306.
[9] M. Akeson, M. Nordberg, A. Ehlerding, L.E. Nilsson, H. Ostmark, P. Strömbeck, Proc. SPIE. 8017 (2011) 1–8.
[10] Y. Fleger, L. Nagli, M. Gaft, M. Rosenbluh, J. Lumin. 129 (2009) 979–983.
[11] J. Moros, J.A. Lorenzo, P. Lucena, L.M. Tobaria, J.J. Laserna, Anal. Chem. 82 (2010) 1389–1400.
[12] J. Moros, J.A. Lorenzo, J.J. Laserna, Anal. Bioanal. Chem. 400 (2011) 3353–3365.
[13] A. Pettersson, S. Wallin, H. Östmark, A. Ehlerding, I. Johansson, M. Nordberg, H. Ellis, A. Al-Khalili, Proc. SPIE. 7644 (2010) 1–12.
[14] J. Fulton, Proc. SPIE. 8018 (2011) 1–7.
[15] S. Wallin, A. Pettersson, H. Östmark, A. Hobro, Anal. Bioanal. Chem 395 (2009) 259–274.
[16] A. Ehlerding, I. Johansson, S. Wallin, H. Östmark, Int. J. Spectrosc. 2012 (2012) 1–9.
[17] W. Ortiz-Rivera, L.C. Pacheco-Londonõ, S.P. Hernández-Rivera, Sens. Image 11 (2010) 131–145.
[18] A.J. Hobro, B. Lendl, Trend Anal. Chem. 28 (2009) 1235–1242.
[19] K. Buckley, P. Matousek, Analyst 136 (2011) 3039–3050.
[20] M. Kim, H. Chung, Y. Woo, M. Kemper, Anal. Chim. Acta 579 (2006) 209–216.
[21] R.F. Bonner, R. Nossal, S. Havlin, G.H. Weiss, J. Opt. Soc. Am. 4 (1987) 423–432.
[22] P. Matousek, Appl. Spectrosc. 61 (2007) 845–854.
[23] B. Zachhuber, G. Ramer, A. Hobro, E.H. Chrysostom, B. Lendl, Anal. Bioanal. Chem. 400 (2011) 2439–2447.
[24] B. Zachhuber, C. Gasser, E. Chrysostom, B. Lendl, Anal. Chem. 83 (2011) 9438–9442.
[25] E.L. Izake, B. Cletus, W. Olds, S. Sundarajoo, P.M. Fredericks, E. Jaatinen, Talanta 94 (2012) 342.
[26] P. Matousek, I.P. Clark, E.R. Draper, M.D. Morris, A.E. Goodship, N. Everall, M. Towrie, W.F. Finney, A.W. Parker, Appl. Spectrosc. 59 (2005) 393–400.
[27] R. Jason, J. Maher, J. Andrew, J. Berger, Appl. Spectrosc. 64 (2010) 61–65.
[28] N.A. Macleod, A. Goodship, A.W. Parker, P. Matousek, Anal. Chem. 80 (2008) 8146–8152.
[29] U. Utzinger, R.R. Richards-Kortum, J. Biomed. Opt. 8 (2003) 121–147.
[30] M.D. Keller, E. Vargis, N.D. Granja, R.H. Wilson, M. Mycek, M.C. Kelley, A. Mahadevan-Jansena, J. Biomed. Opt. 16 (2011) 077006-1–077006-8.
[31] C. Ricci, C. Eliasson, N.A. Macleod, P.N. Newton, P. Matousek, S.G. Kazarian, Anal. Bioanal. Chem. 389 (2007) 1525–1532.
[32] N. Macleod, P. Matousek, Pharm. Res. 25 (2008) 2205–2215.
[33] W. Olds, E. Jaatinen, P. Fredericks, B. Cletus, H. Panayiotou, E.L. Izake, Forensic Sci. Int. 212 (2011) 69–77.
[34] B. Cletus, W. Olds, E.L. Izake, P. Fredericks, H. Panayiotou, E. Jaatinen, Proc. SPIE. 8032 (2011) 1–13.
[35] R.M. Measures., Fundamentals of laser remote sensing, in: R.M. Measures (Ed.), Laser Remote Chemical Analysis, John Wiley and Sons, New York, NY, 1988, Pp. 1–83.
[36] F. Ariese, H. Meuzelaar, M.M. Kerssens, J.B. Buijs, C. Gooijer, Analyst 134 (2009) 1192–1197.
[37] I.E. Petterson, P. Dvořàk, J.B. Buijs, C. Gooijer, F. Ariese, Analyst 135 (2010) 3255–3259.
[38] J. Blacksberg, J.R. Rossman, A. Gleckler, Appl. Opt. 49 (2010) 4951–4962.
[39] Y.A. Tobon-Correa, A. Bormann, A. Canizares, N. Raimboux, P. Simon, J. Raman Spec 42 (2010) 1109.
[40] P. Matousek, N. Everall, M. Towrie, A.W. Parker, Appl. Spectrosc. 59 (2005) 200–205.
[41] E.I. Petterson, M. Lopez-Lopez, C. Garcia-Ruiz, C. Gooijer, J.B. Buijs, F. Ariese, Anal. Chem. 83 (2011) 8517–8523.
[42] B. Zachhuber, C. Gasser, G. Ramer, E.H. Chrysostom, B. Lendl, Appl. Spectrosc. 66 (2012) 875–881.
[43] B. Cletus, W. Olds, E.L. Izake, S. Sundarajoo, P.M. Fredericks, E. Jaatinen, Anal. Bioanal. Chem. 403 (2012) 255–263.
[44] B. Cletus, W. Olds, E.L. Izake, S. Sundarajoo, P.M. Fredericks, E. Jaatinen, Proc SPIE 8374 (2012) 837403-1–837403-7.
[45] E.V. Efremov, J.B. Buijs, C. Gooijer, F. Ariese, Appl. Spectrosc. 61 (2007) 571–578.
[46] N. Everall, T. Hahn, P. Matousek, A.W. Parker, M. Towrie, Appl. Spectrosc. 55 (2001) 1701–1708.
[47] P. Matousek, M. Towrie, C. Ma, W.M. Kwok, D. Phillips, W.T. Toner, A.W. Parker, J. Raman Spectrosc. 32 (2001) 983–988.